Advanced Centre for Atmospheric Sciences

Sponsored by
Dept. of Space, Govt. of India

Prof. S. Vijaya Bhaskara Rao
Co- Ordinator

Progress Report

Department of Physics
S. V. U. College of Sciences
S. V. University
Tirupati-517502

1. General Information

1.Project Title:	**Advanced Centre for Atmospheric Sciences**
2.Principal investigator with address	**Dr. S. Vijaya Bhaskara Rao** Professor, Department of Physics S. V. University, Tirupati-517502
3. Other Investigator(s) with address(es)	Nil
4. Period of the Project (with Starting Date and Completion date)	**1st April 2015 to 31st December 2020**
5.Total grant approved/released by ISRO	Rs.75.71 lakhs
	Rs.13.13 lakhs(1st year grant released) Rs.18.84 lakhs (2nd year grant released) Rs.15.88 lakhs (3rd year grant released) Rs.14.49 lakhs (4th year grant released) Total: Released Rs.62.34 lakhs
6. Major equipment procured	Nil
7.Name of the ISRO/DOS Centre involved	National Atmospheric Research Laboratory (NARL), Gadanki
8. Names and present addresses of Research Fellows who worked in the Project	**Dr. G. N. Madhavi** National Post-Doctoral Fellow Vignana bharathi institute of technology Hyderabad **L. Ramanjaneyulu**, PhD Student EECS International Graduate Program National Chiao Tung University, Taiwan
9. Names and present addresses of Research Associates/other research Staff recruited for the project	**Dr. Prabodha Kumar Pradhan** Research Associate Dept. of Physics, S V University, Tirupati. prabodhakumar@gmail.com **K. Vijaya Kumari** Senior Research Fellow Dept. of Physics , S.V.University , Tirupati (completed) Ph.D. in March 2021

	K. Vishnu Vardhan Reddy Senior Research Fellow Dept. of Physics , S.V.University , Tirupati
10. Broad area of Research:	**Atmospheric Science**

2. Ph. D degree awarded during 2015-2021:

1. **Miss Madhavi Gummadipudi on the topic "**Global Temperature Morphology and planetary wave characteristics using different satellite measurements" under Prof. S. Vijaya Bhaskara Rao, December, 2015
2. **Miss. K. VijayaKumari** on the topic "Simulation of tropical cyclones over Bay of Bengal using WRF-ARW model: sensitivity of planetary boundary layer, air-sea processes and data assimilation" under Prof. S. Vijaya Bhaskara Rao, March, 2021
3. **K.Vishnu Vardhan Reddy** on the topic "Slant path rain attenuation prediction for Ku and Ka band frequencies from rain cell size distribution over a tropical region in Southern India**"** under S. Vijaya Bhaskara Rao **(To be submitted)**

3. Objectives of the Proposal:

1. Low latitude Mesosphere Dynamics
2. Monitoring of Atmospheric aerosols and analyzing their impact on climate
3. Direct and indirect effects of aerosols on Indian Monsoon
4. Prediction of rainfall (inclusive of monsoon and tropical cyclones) and high impact weather events over India using high resolution weather prediction models.
5. Monitoring of Atmospheric Parameters using GPS-RO technique

4. Major Results and discussion

4.1. A case study of convectively generated gravity waves coupling of the lower atmosphere and mesosphere-lower thermosphere (MLT) over the tropical region: An observational evidence

Introduction:

It is well understood that the atmospheric gravity waves (GWs) are playing a vital role in understanding the structure and dynamics of the middle atmosphere. GWs are most significant in transporting energy and momentum from the lower to the middle and upper atmosphere, and most of the GW sources are located in the troposphere. Though the long-period and short-period GWs exist in the atmosphere, the long-period GWs are influenced by the rotation of the earth and the geostrophic adjustment process can act on the ageostrophic component in synoptic-scale wind systems, but the short-period GWs are believed to be generated locally. Further, the GWs gained its importance in changing the MLT thermal structure. It was understood that GWs are the potential constraints in the changing mesosphere temperature and causes the Mesosphere Temperature Inversion (MTI) and the turbulence below and above the inversion layer. The aim of this study is to investigate the vertical coupling process by the short-period GWs using the two active ground-based instruments (MST Radar and LIDAR) and quantifying the amount of GW fluxes transported from the lower atmosphere to the mesosphere, during the deep convection.

Results:

To understand the wave forcing from the lower atmosphere to the mesosphere, we further looked into the tropospheric vertical velocities observed by MST Radar and Rayleigh LIDAR temperature profiles in the upper stratosphere and lower mesosphere during the deep convection day. Fig.1a shows the Lomb-Scargle (L-S) periodogram analysis of the tropospheric vertical winds obtained from the MST Radar at 10, and 16 km, respectively. Fig.1b displays the Rayleigh LIDAR daily mean temperature profiles with each profile shifted by 20K for clarity. Since the LIDAR was not operated continuously during the convection period due to bad weather, we could not get time series profiles. The L-S periodogram analysis in the troposphere shows that the short-period GWs (20min-2h) is evidenced during the convection day and their amplitudes are observed above the confidence level, specifies the waves are generating in the troposphere due to deep convection. The daily mean night-time LIDAR temperature profiles (Fig.1b) during the convection day and normal days, clearly reveals the signature of GWs in temperature perturbations from 50-75 km during the deep convection day. In contrast, such features are not seen on normal days. This aspect further supports the existence of the strong link between the lower atmosphere and mesosphere through the GWs, generated by the convection.

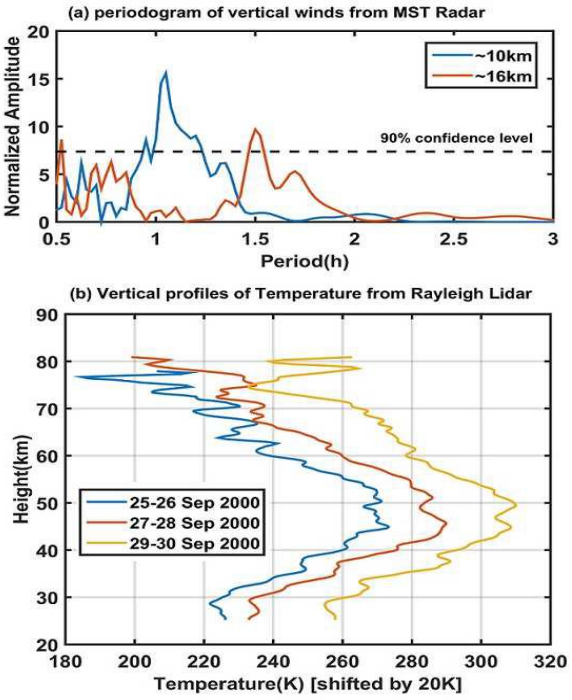

Fig. 1 (a) Lomb–Scargle periodogram analysis of tropospheric vertical winds obtained using MST Radar at 10, and 16 km, respectively.
(b) Rayleigh LIDAR daily mean temperature profiles shifted by 20K.

Due to clouds and bad weather during the convection day, LIDAR has not been operated continuously and hence we could not get time series data in the gap region (30-60 km) to show the GW features. But, the mean profile clearly reflects the wave features. To determine the GWs breaking and deposition of energy and momentum at the mesosphere altitudes, we have estimated the amount of momentum flux carried by the GWs to the mesosphere and their momentum flux in the troposphere. The time variation of vertical flux of zonal and meridional momentum flux on the convection day is presented in Figure 2.

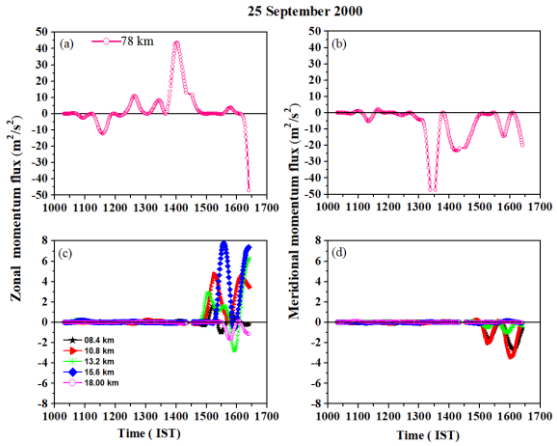

Fig. 2 Zonal (left panels) and meridional (right panels) momentum fluxes at different altitudes observed on 25 September 2000 in the troposphere (bottom panels) and the mesosphere at 78 km (top panels).

The fluxes are evaluated and averaged over about 15 min. During the peak convection time (1500h-1630h IST), the momentum flux in the tropospheric altitudes is significantly higher with the mean magnitudes of ~ 3 m^2/s^2 and even more. Much of the time, the zonal momentum flux is eastward (Fig.2c) and meridional momentum flux is southward (Fig.2d) in the troposphere. At the mesospheric altitude (78 km), the zonal momentum flux values are perturbed from mean values even before the convection. This might be associated with the GWs propagating radially from the convection plumes existed adjoining to the observational site. The momentum flux values both in the zonal (Fig. 2a) and in the meridional wind (Fig.2b) reached up to $45m^2/s^2$.This higher momentum fluxes further indicate the amplitude of GWs increases exponentially in vertical as the density decreases. It is obvious from Fig. 2, that both the zonal (Fig.2a) and meridional fluxes (Fig.2b) in the mesosphere shows large values even before the convection event over Gadanki region, and also peak convection hours. This is probably due to the waves generated by convective region elsewhere and also at the Gadanki. This is the unique observational study over the tropical region, India, and shows the signature of vertical coupling of the lower atmosphere and mesosphere through short-period GWs.

This work is published in Journal of Atmospheric and Solar-Terrestrial Physics.
DOI: 10.1016/j.jastp.2018.01.005

4.2 Effects of agriculture crop residue burning on aerosol properties and long-range transport over northern India: A study using satellite data and model simulations

Introduction

Agriculture crop residue burning in tropics is a major source of the global atmospheric aerosols and monitoring their long-range transport is an essential element in climate change studies. The *agricultural crop residue burning that* takes place in the Indo-Gangetic Plains *(IGP) in Northern Indian region* has been reported to contribute substantially to the overall aerosol loading over this area. The aerosol properties in this region are severely affected by *agricultural crop residue burning* particularly during the months of October and November every year, which is the rice harvesting period in North India. The main objective of the present study is to analyze the variations in aerosol optical properties associated with agricultural crop residues burning in IGP using satellite data sets along with model simulations. The satellite observations during 09-17 November, 2013 have been used in this study.

Results

MODIS true color fire image of 12 November 2013 with approximate locations of the active burning image along with ECMWF derived winds at 850 hPa during 12-14 November 2013 is shown in Fig. 1.

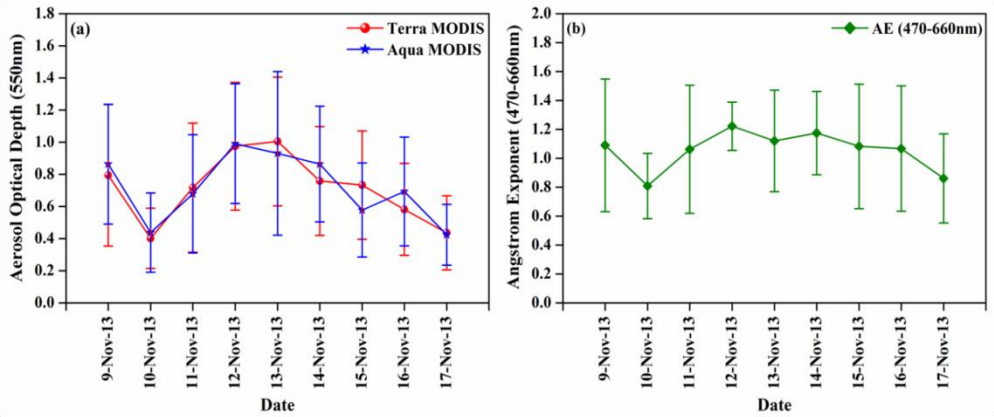

Fig 1. (a) MODIS Aqua satellite true color image of fires over Punjab state on 12 November 2013, (b) selected stubble burning region, (c) MODIS Terra and Aqua satellite combination of fire image on 12 November, and (d) ECMWF derived winds at 850 hPa over Indian region during 12–14 November 2013.

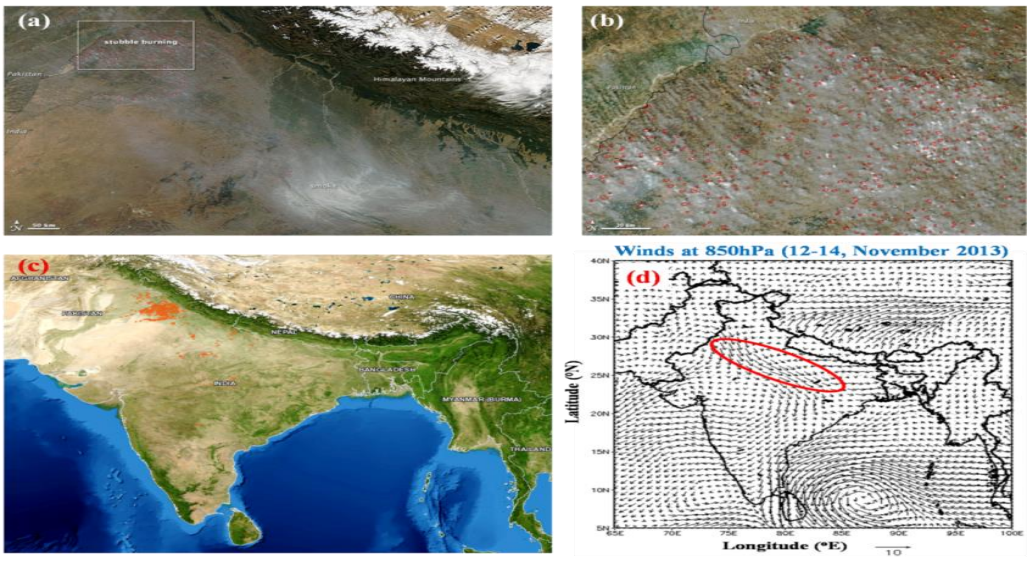

Fig. 2. Day to day variation of (a) AOD at 550nm, and (b) AE at 470-660nm.

The increase in fine mode particles loading, due to long range transport of aerosols from BB reflected in an increase of aerosol optical depth (AOD) and Angstrom exponent (α) on 12

November compared to that on 11 November (see Fig. 2). It can be seen from both Fig. 2(a) and 2(b) that higher values are observed on 12 November 2013, suggesting an abundance of fine mode particles in the atmosphere. The higher (~ 51.08%) AE (fine-mode aerosols) values together with high AOD values are attributed to the presence of BB aerosols over the study region.

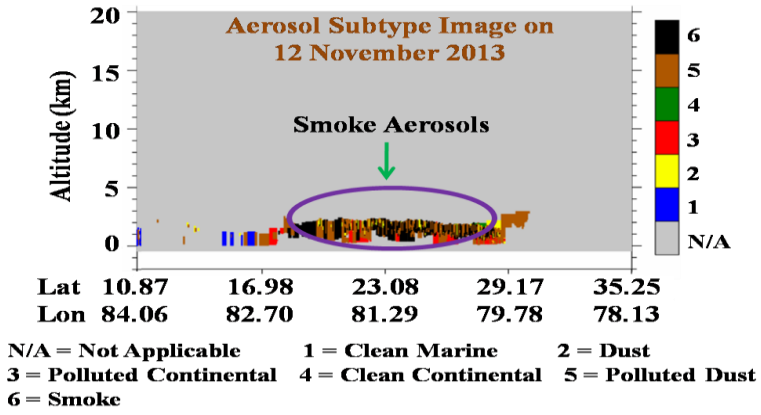

Fig. 3. Day to day variation of Dust, OC, and BC AODs derived from ECMWF MACC reanalysis during study period.

The relative variations of ECMWF MACC reanalysis parameters such as dust, OC, and BC AODs are shown in Fig. 3. It is again clearly seen that all AODs show higher values during smoke event period. Especially dust AOD dominated other AODs. It is ~78.5% higher on 12 November 2013 (high aerosol loading day) compared to 10 November 2013 (normal day). The OC and BC AODs are higher up to 13 November 2013 due to finer aerosols and these are stable in the atmosphere. These OC and BC AODs are ~139.5% and ~101.6% higher on 13 November 2013 compared to 10 November 2013.

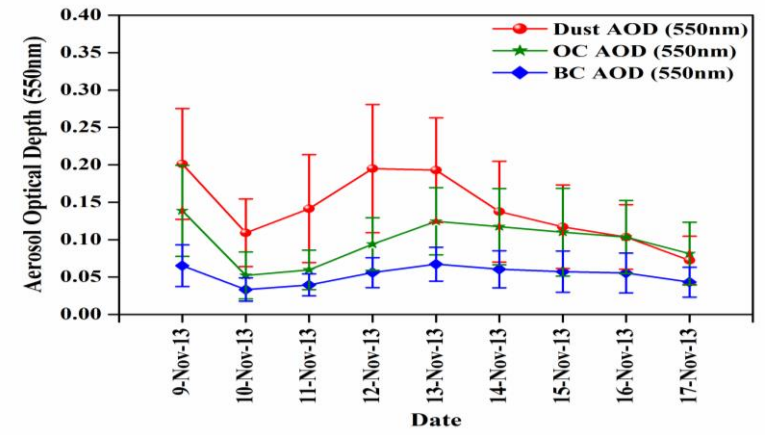

Fig. 4. Aerosol subtype image obtained from CALIPSO observations on 12 November 2013.

The other study of the nearest CALIPSO pass available on 12 November 2013, covering north east part of the Indian region. Figure 4 shows aerosol subtype image on 12 November 2013. The aerosol subtype image, as revealed by the lidar back-scatter, highlights the signals into 7 categories. The category 6 (in black) has a greater importance as well as the presence of smoke aerosols. It clearly shows a layer of thick smoke extending from surface to an altitude of about 3 km. The plot clearly shows continental pollution consisting of smoke and dust particles on the observational day over the study region. The combined effect of polluted dust and smoke aerosols seems to be an increase in cloud cover with increasing aerosol column concentrations.

This work was published in Atmospheric Research, 2016, Vol no: 178-179, Page no: 155-163, Impact Factor: 2.84.

4.3 Dust aerosol characterization and transport features based on combined ground-based, satellite and model-simulated data

Introduction

Dust is a global phenomenon, and it impacts regional/global climate and the biogeochemistry of land and oceans. The Arabian Peninsula is one of the most difficult environments to characterize, monitor and model as it is the largest confluences of dust and anthropogenic emissions in the world. Frequent dust storms and high pollution levels are main features of the region. Once dust is raised, its direction of transport depends on prevailing wind direction and speed. Therefore, the transport of dust aerosols plays an important role in the regional and global radiative balance both at the surface and the top of the atmosphere. Dust monitoring can better be achieved by the combined use of the satellite and ground-based

observations, and model simulations provide further understanding and prediction capabilities. The dust aerosol plume that originated over the Arabian Sea during 18–20 March 2012 over Pune, an urban area located at about 100km inland from the west coast of India. It persisted from 21 to 25 March 2012. The source and characteristics of data sets, archived from ground-based, space-borne experiments and model evaluations.

Main results of the study:

Figure 1(a) shows the MODIS Terra and Aqua satellite image of the major dust plume during 18–20, March 2012 that covered an extremely large area and disrupted human activities in Iraq, Iran, Kuwait, Syria, Jordan, Israel, Lebanon, UAE, Qatar, Bahrain, Saudi Arabia, Oman, Yemen, Sudan, Egypt, Afghanistan, and Pakistan. The variations in AERONET products (AOD (Aerosol Optical Depth) at 440 nm, Fine Mode (FM) and Coarse Mode (CM) AOD at 500 nm, Ångström exponent (440–870 nm), and Fine Mode Fraction (FMF) at 500 nm) before, during and after occurrence of the dust event are shown in Figure 2(a–d), respectively. As shown in Figure 16(a), the AOD at 440 nm values increase progressively from 18 to 20 March, exhibiting the highest value (~0.8) on 21–23 March (major intensity of the dust event). Thereafter, the AOD progressively decreases, but at a lower rate, since the thick dust layer emitted in the middle and upper atmosphere can stay over there for several days. The larger standard deviation on 21 March indicates the significant spatial distribution in aerosol load over the area caused by the intense dust storm. The FM and CM AOD variation (Figure 16(b) clearly shows during dust event period CM AODs are dominated compared to FM AODs due to abundance of coarse dust particles are transported from Arabian Sea. The Ångström exponent and FMF (Figure 16 (c and d) values clearly indicate the dominance of coarse-mode aerosols during the study period.

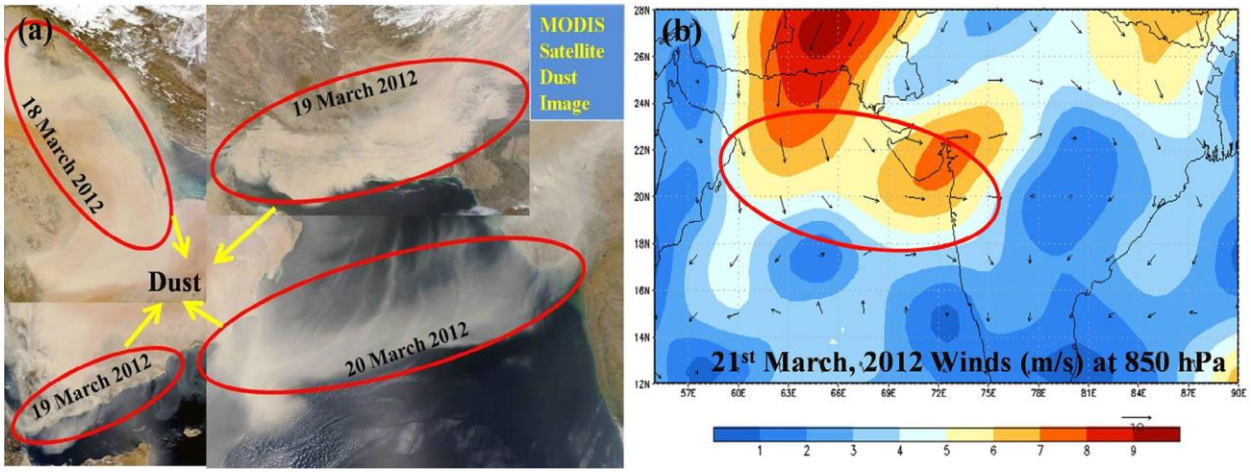

Fig 1 (a) The MODIS satellite image during March 2012, showing the transport of dust plume across the Arabian Sea to reach India and **(b)** Spatial distribution of wind speed and direction at 850 hPa on 21 March 2012 over south Asia derived from NCEP/NCAR reanalysis.

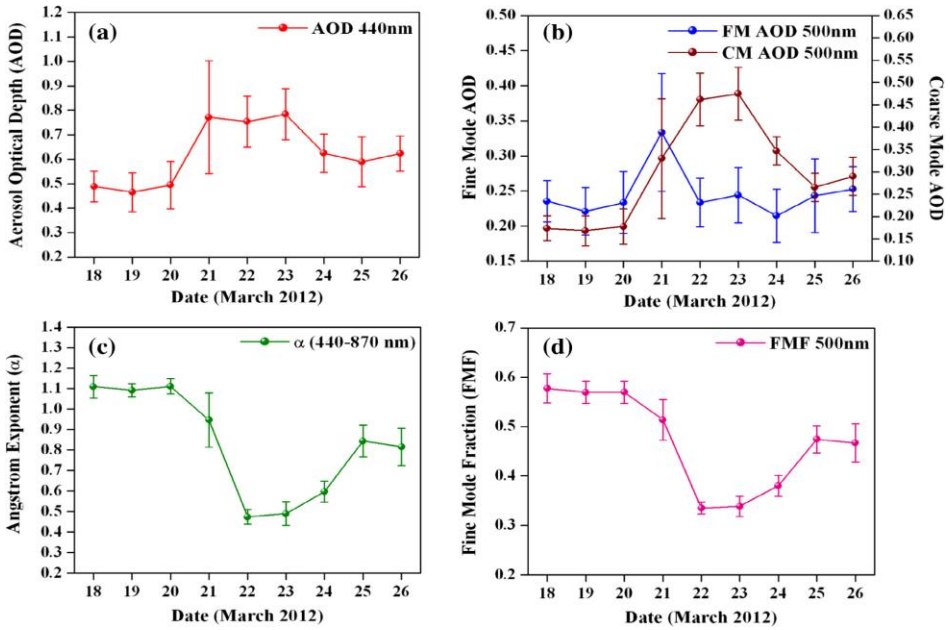

Fig. 2. Daily variation of the AERONET AOD at 440 nm (a), fine mode and coarse mode AOD at 500 nm (b), Ångström exponent a in the spectral band 440–870 nm (c), and fine mode fraction at 500 nm (d) over the experimental site. The vertical bars show one standard deviation from the mean area-averaged value.

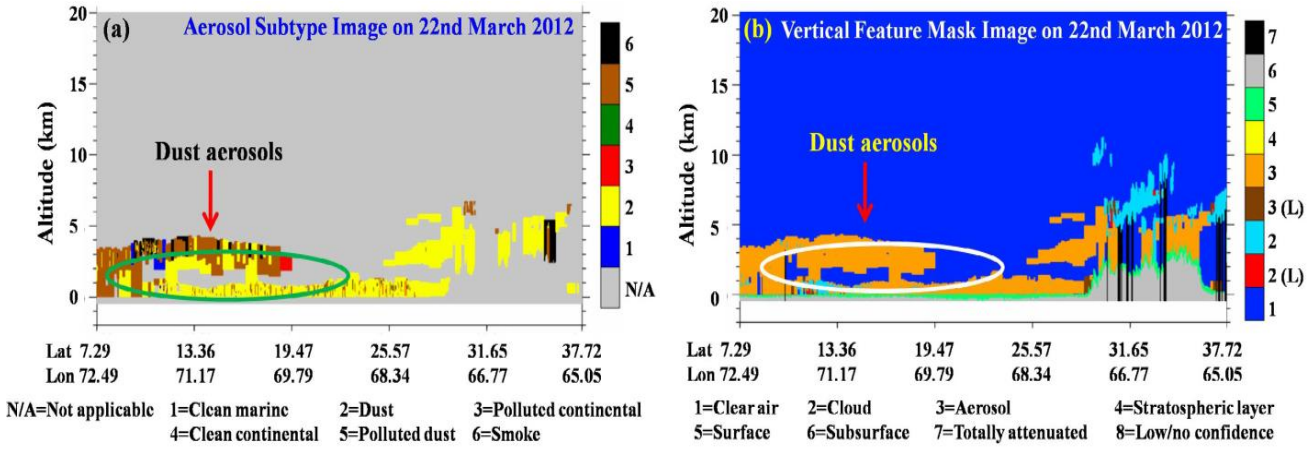

Fig 3. (a) CALIPSO retrieved aerosol classification (sub-type profile), and **(b)** vertical feature mask on 22 March 2012 over the studied region.

A typical example of the vertical distribution of the dust plume over the study region during daytime on 22 March 2012 is shown in Fig. 3 (a and b). The aerosol subtype profile from CALIPSO measurements on the same day is shown in Fig 17(a). This figure reveals that a well-mixed dust layer occurred over the Pune area in India (closest CALIPSO approach approximately 100–200 km). The aerosol types identified by CALIPSO in the vicinity of the study region include both dust and polluted dust, but dust aerosols were dominant over the anthropogenic (polluted) aerosols. The CALIPSO aerosol profiles indicated a layer of thick dust

(carrying coarser particles) extending from the surface to an altitude of about 4 km (see Fig. 3 (a)). The high aerosol concentrations over Pune may therefore have been due to dust transported from afar, with lesser contributions from local sources. Added, vertical feature mask image shows clearly dust layer development over the northeastern part of the Arabian Sea extended from the ground level to a height of 3–4 km during day time conditions (Fig. 17(b)). These results reveal that the recent developments in satellite remote sensing technique revolutionized the aerosol monitoring, and providing tremendous application in the identification of the dust sources, vertical extent and pathways.

This work was published in Aeolian Research, 2016, Vol:21,75-85.
DOI:10.10.16/j.aeolia.2016.03.003. Impact Factor 2.31

4.4 Impact of Assimilating SCAT SAT-1 data on tropical cyclone simulation of Cyclone "Vardah"

Introduction

In order to get the information about cyclone structure which includes eye, eye wall, spiral bands organisation etc and its propagation, it is necessary to accurately build up the wind information in the initial conditions to the models. The vortices of TCs at the starting phase can be easily resolved by accurate knowledge of surface winds which is a difficult task for numerical model. Due to the lack of observations over ocean, the understanding of the active region of the cyclone formation is difficult and hence limits the prediction. Therefore synoptic methods and satellite remote sensing are the best options to predict the track of the cyclones. Numerous satellite data is available now days, so that the assimilation of wind information can be done to initialise the models precisely. The WRF-ARW model is initialized with the NCEP-FNL 1˚×1˚ resolution data. FNL 6-hourly is used for the simulations of cyclone parameters. Two domains are selected for the experiment. Parent domain covering the major Asian land regions and North Indian Ocean basin with 27kms horizontal grid resolution. Inner domain with 9km resolution covers the BOB and Indian land regions. The model simulations are carried out by fixing the best combination of microphysics, surface clay, boundary layer and cumulus parameterization schemes mentioned in the recent studies of model sensitivity to physics parameterizations in predicting the tropical cyclones. Simulations are carried by assimilating the SCATSAT data into PrepBUFR global observations from the NCEP using WRFDA.

Results

One recent tropical cyclone formed over Bay of Bengal in 2016 is selected i.e., cyclone "Vardah" for the analysis in depth. As the SCATSAT-1 was very recently launched, very few studies are carried out. Scatterometer derived winds from SCATSAT-1 are assimilated using WRF model and few experiments are carried out to refine the predictions of the cyclone. The main objective is to prepare the numerical model efficient enough at the starting phase of the TC to achieve minimal error. The vortices of the cyclonic storm from the knowledge of scatterometer data are corrected and the predictions are carried out. Fig. 1 represents the scatter

plots before (left panel) and after (right panel) appending the SCATSAT (right panel) in the initial condition. Successful assimilation reduces the departures of analysis from observations relative to the departures of first guess from observations, thereby bringing the analysis towards observations.

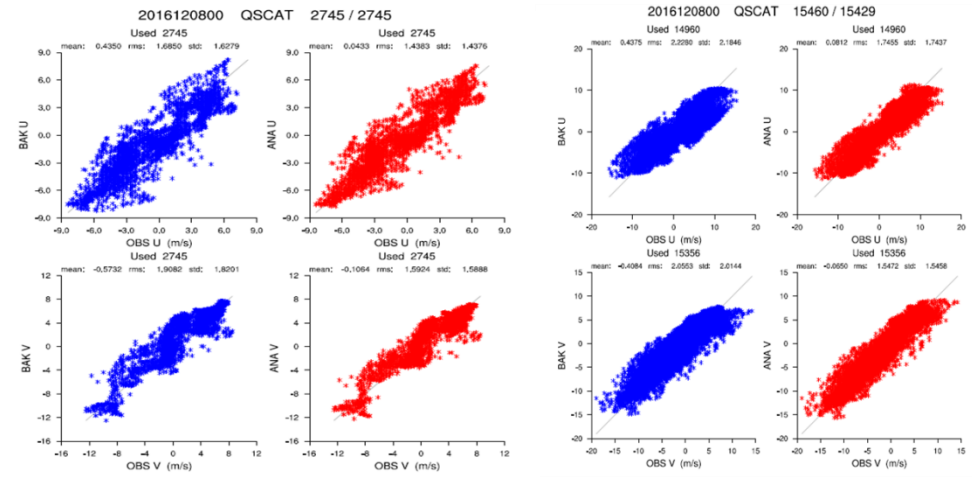

Fig 1. Scatter plot of observations versus first guess (in blue) and 3D-Var analysis (in red) for U wind and V wind corresponding to the analysis time 00:00 UTC 9 October 2013.

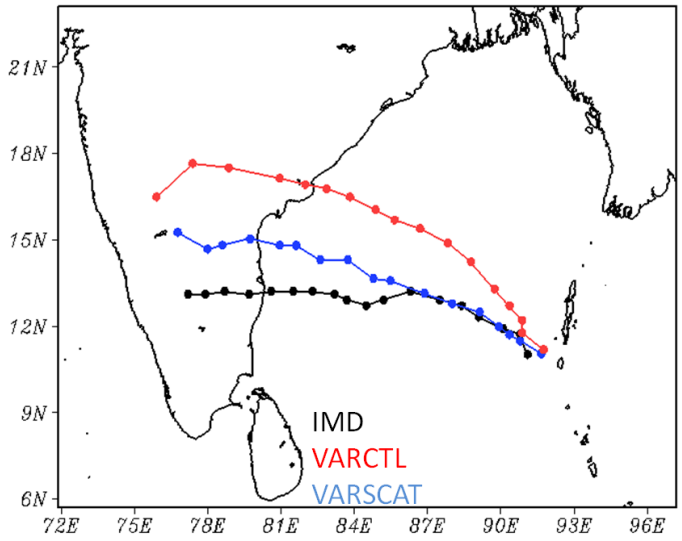

Fig.2 Comparison of simulations of Vardah Vector track positions with IMD best track data.

Notable changes in the track positions are recognized by assimilating the SCATSAT data as shown in Fig. 2. Intensity of the cyclone is also in agreement with the IMD estimates. Even more analysis and further investigation is needed to support this study.

4.5 Impact of Ocean Mixed Layer Depth Initialization on simulation of tropical cyclones over Bay of Bengal using WRF-ARW model

Introduction:

In this study, Advanced Research WRF (ARW) version 3.9.1 and in built simple Ocean Mixed Layer (OML) (WRF-OML) are used to analyze the impact of mixed layer dynamics on simulation of Tropical Cyclone (TC) over Bay of Bengal (BOB). The details of the WRF-OML system can be obtained from Mohan *et al*., 2015. The modeling system is configured with two nested domains with 27 and 9 km horizontal resolutions covering the BOB and its adjoining regions, the high resolution inner domain covers the BOB and the east coast of India. The first domain with 27km covers the Indian Sub-continent and North Indian Ocean basin same as in Vijaya Kumari *et al*., 2018; Srinivas *et al*., 2013. The model physics used in the study are adopted, from the previous modelling studies on physics sensitivity in predicting the TCs over BOB. The initial conditions are provided from the Global Forecast System (GFS) 0.5°× 0.5° resolution analysis from analysis of National Center for Environmental Prediction (NCEP) and boundaries are updated at 6-hourly interval. The ocean initial conditions for the WRF-OML system are obtained from reanalyzed data of HYCOM.

Results

Four sets of numerical simulations are performed for the two TC cases by initializing the model at 1200 UTC 28 April 2008 and 0000 UTC 09 December 2015and integrated up to 120 hours for Nargis and Vardha respectively. In the first experiment (CONTROL), along with GFS analysis, the lower boundary SST fields are replace by time varying fields of high resolution Real-time Global (RTG) SST, and other three experiments are conducted by incorporating coupling feedback of OML physics through WRF-OML system in each TC case. Out of three WRF-OML experiments, the first WRF-OML experiment is configured with constant Mixed Layer Depth (MLD) of 50 m (MLD-CONST) and in the second experiment (MLD-TEMP), the coupled system initialized with spatial variation of MLD computed based on the isothermal temperature profiles of HYCOM dataset, while in the third WRF-OML experiment (MLD-DENS), the initial values of MLD are replaced with density based MLD obtained from the 3D thermohaline field (ARMOR 3D level 4 data). The MLD is computed based on the variable density criteria, the depth at which density has varied significantly to the surface value by threshold value of 0.2 °C (de Boyer Montégut, 2004). More details about the density based MLD dataset can be found in Buongiorno, 2017.

The initialization of the different estimates of MLD (shown in Fig. 1) in WRF-OML shows the TC intensity and translation speed are sensitive to the initial representation of MLD for the post-

monsoon storm, but these initial variations of MLD shows little impact on the simulation of vector tracks. The gradual improvements in the intensity and translation speed of the storm with the realistic representation of OML are mainly due to the storm induced cooling which changes in the enthalpy fluxes supplied to TC, leading the better representation of secondary circulation and the evolution of deepening phase of the storm. When an intensified cyclone pass through a shallow mixed layer, storm induced strong winds lead to the upwelling of the ocean waters from sub-surface to cool the surface ocean waters, leading to a decrease in Sea Surface Temperature (SST) during the passage of the cyclone, which in turn acts like a negative feedback of ocean to reduces the flux feedback to suppress the intensification of Tropical Cyclone (Mao *et al*., 2000). To present the storm induced SST cold wake, the simulated SST anomaly (shown in Figure 10) computed between the SST's at the time of model initialization and after the TC passage, along with the corresponding microwave SST obtained from Special sensor microwave imager (SSMI) is presented. The SSMI SST's clearly indicating the storm induced cooling (> 1.5 °C) for the both TCs to the right side of the cyclone track. While the results of simulated cold wake in both TC cases indicate that when the spatial variation of MLD is set to constant (50 m) in the initial conditions (MLD- CONST), though SST cooling is observed along the right side of the storm track, the magnitude is found to be less (0.25 °C to 0.5 °C) compared to the other WRF-OML simulation.

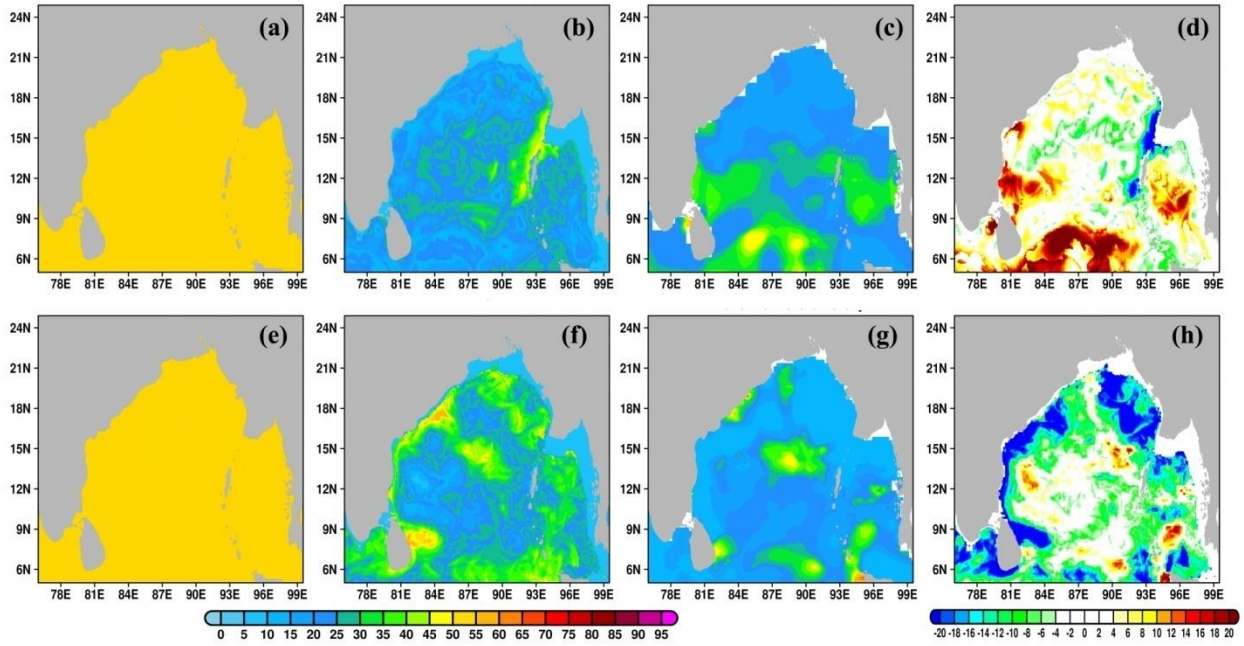

Fig. 1: Spatial distribution of mixed layer depth (m) during the model initialization for Nargis at 1200 UTC 2008 (top panels) and Vardah at 0000 UTC 09 December 2016 (bottom panels) from (a, e) MLD-CONST, (b, f) MLD-TEMP (c, g) MLD-DENS and (d, h) differences in MLD-TEMP and MLD-DENS.

The magnitude of the storm induced SST cooling is slightly increased from 0.5 °C to 0.75 °C when the initial MLD obtained spatially from Isothermal Layer Depth (MLD-TEMP). The magnitude of the storm cooling (> 1.25 °C) is significantly increased and a well-marked pattern is observed on the right side of the cyclone track in the simulation of MLD computed from density (MLD-DENS). Simulation of storm induced SST is one of the prominent parameter for the coupled model simulations for TC. The results indicated that the simulated SST cold wake obtained from MLD-DENS realistically captured the observed pattern of SSMI SST product in both the cyclone cases.

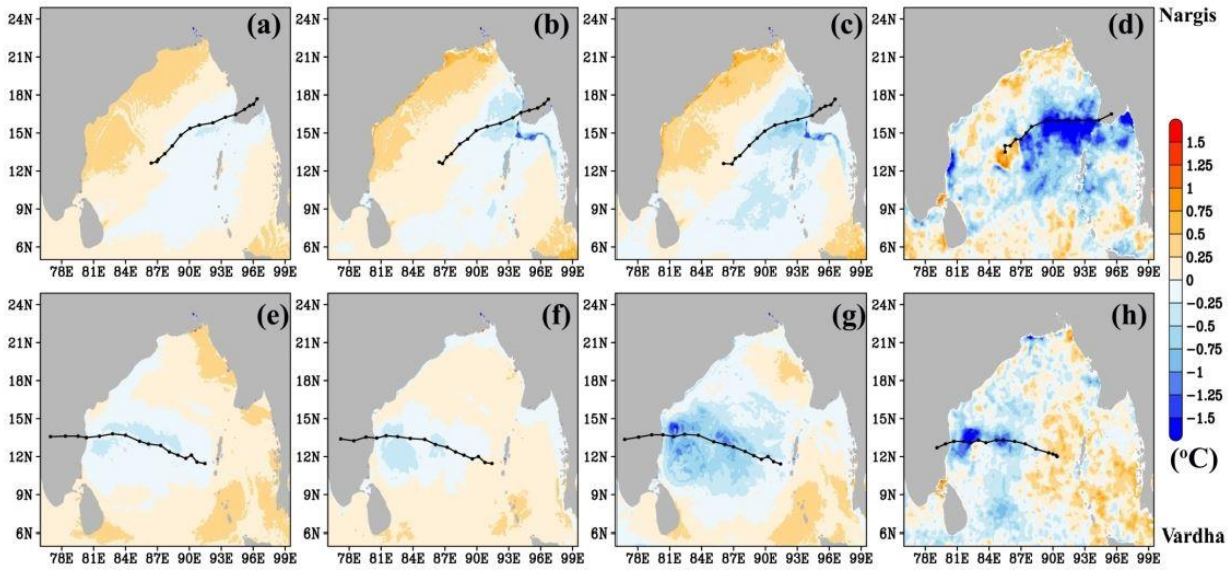

Fig. 2: Comparison of simulated SST anomaly (°C) from a & e) MLD-CONST, b & f) MLD-TEMP and c & g) MLD-DENS with d & h) corresponding SSMI merged product for TC Nargis at 12 UTC 2 May 2008 (top panels) and vardha (bottom panel) at 12 UTC 12 December 2016.

This work is published in Meteorological Applications in October 2019
[Impact factor 1.411]

4.6 Simulation of mid-latitude storms over the North Atlantic Ocean: impact of boundary layer parameterization schemes

Introduction

The mid-latitude winter storms affect several countries in western and northern Europe and widespread gusts reaching 111–129 km h^{-1} across south-east England, which was recorded as one of the strongest autumn storms in the region, since 2002. Well studied mid-latitude winter storms such as Klaus, Xynthia, Gong, and Stephanie stroke directly to the Iberian Peninsula (IP) and moved further eastward characterized by the lowest MSLP of <963 hPa which produced strongest winds, leading losses in Europian region.. This study discusses the performance of

various planetary boundary layer parameterization (PBL) schemes-the Quasi-Normal Scale Elimination (QNSE), the University of Washington Moist Turbulence (UWMT), and the Yonsei University (YSU)—for the simulation of rapidly developing North Atlantic (NA) mid-latitude winter storms. Sensitivity experiments with the three PBL schemes, YSU, QNSE, and UWMT, indicate that there are minor differences at the center of the storm while simulating the evolution of the three explosive storms Klaus (21–27 January 2009), Xynthia (25 February–03 March 2010), and Gong (16–20 January 2013). One of the main results shows the capability of QNSE and UWMT PBL schemes to reproduce accurately both the cyclogenesis and explosive stage for these mid-latitude storms during the winter season, better than YSU scheme.

Results

The WRF mesoscale model developed by the National Center for Atmospheric Research (NCAR), USA is used for the real-time simulations of mid-latitude storms in this study. It is a mass conservative finite difference model and uses non-hydrostatic compressible Euler equations, terrain-following hydrostatic pressure vertical coordinate and Arakawa-C type horizontal grid (Skamarock et al., 2008). In this study the WRF model is configured with 2-domains of horizontal resolutions 25 km and 8.333 km. The inner finer domain covers the entire region of IP.

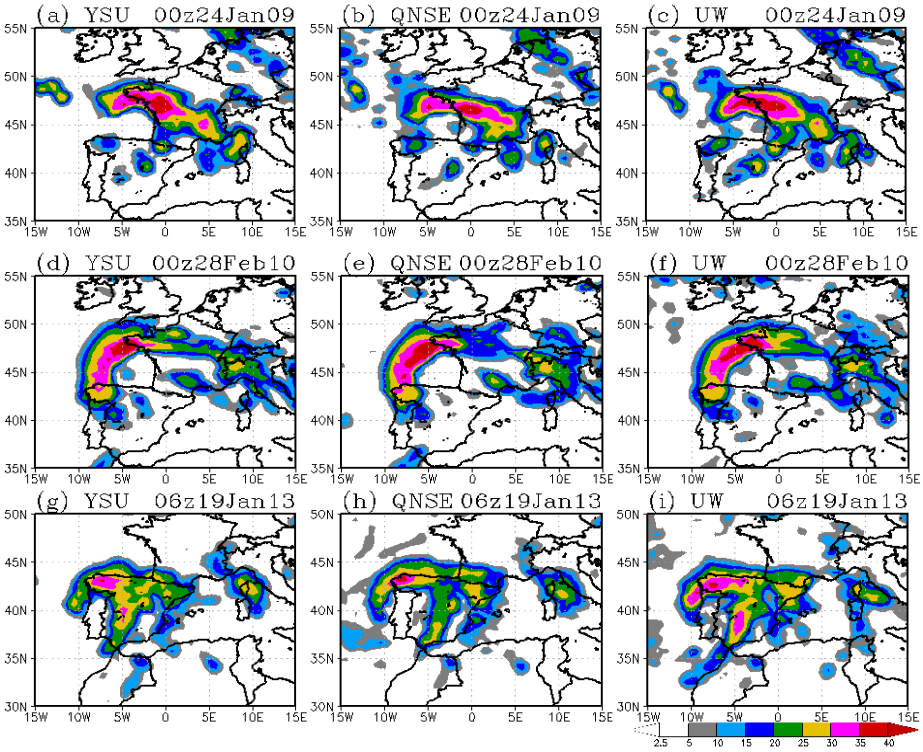

Fig. 1 Reflectivity (dbz: shaded) of mid-latitude cyclones Klaus during mature stage simulated by using (a) YSU, (b) QNSE, and (c) UW experiments valid on 00UTC 24 January 2009. Similarly, mature stage of Xynthia (d) YSU, (e) QNSE, (f) UW and Gong (g) YSU, (h) QNSE, (l) UW PBL experiments.

Model physics includes Kain–Fritsch scheme (Kain and Fritsch, 1993) for convection, WRF Single Moment (WSM6) scheme for cloud microphysics (Hong and Lim, 2006), NOAH scheme (Chen et al., 2001) for land surface processes, RRTM scheme (Mlawer et al., 1997) for long-wave radiation and Goddard scheme for shortwave radiation (Chou et al., 1994). The same convection scheme is employed for the higher resolution domain D02. Three PBL schemes YSU, QNSE and UWTM PBL physics of three storms considered in this study. Reflectivity measures the type of prognostic water substance variables such as precipitation (includes mixing ratio of water vapour, cloud water, cloud ice, snow, rain, and graupel), a cyclone carries during a course of time (Figure 1). Some of the PBL scheme show an elongated and widespread reflectivity for cyclones e.g. YSU for Klaus, QNSE for Xynthia and UW for Gong.

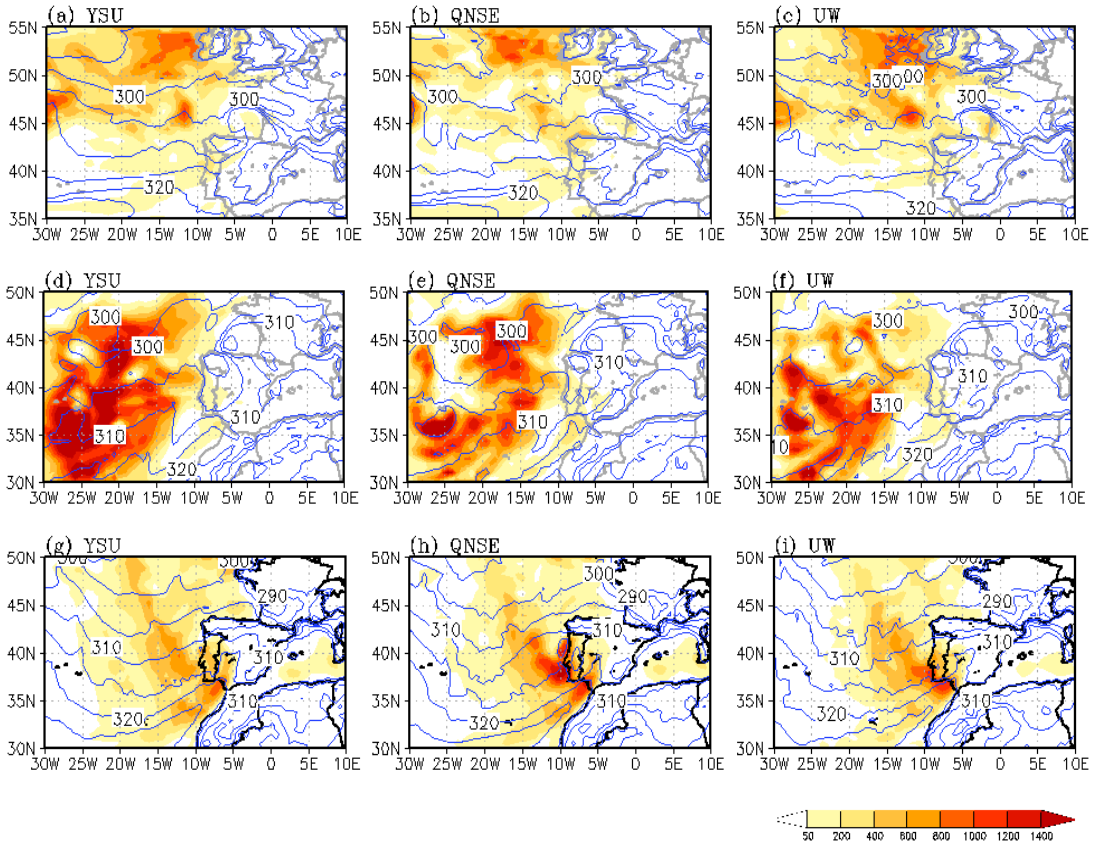

Fig. 2 Simulated convective available potential energy (CAPE) (shaded; JKg) and equivalent potential temperature (blue; contours) of mid-latitude cyclones Klaus during mature stage simulated by using (a) YSU, (b) QNSE, and (c) UW PBL schemes valid on 00 UTC 24 January, 2009. Similarly, (d-f) for Xynthia valid on 00 UTC 28 February, 2010 and (g-i) for Gong valid on 06 UTC 19 January, 2013 respectively.

A variety of precipitation can be seen in case of Xyntia cyclone which was highly explosive than other two cyclones. Studies by Sobel et al., (2001) documented about the, horizontal temperature gradients are small in the tropical atmosphere, as a consequence of the smallness of the Coriolis

parameter near the equator. Moreover, the situation is very different in mid-latitudes and temperature variations are much larger than tropics. Therefore, the forecasting of hazardous events such as thunderstorms, storms and mesoscale convective systems in mid-latitude the temperature gradients is quite important for large contribution to the variation of CAPE (Yano et al., 2013).

The modification of the PBL height should affect the convective available potential energy (CAPE) and convection by modulating the vertical distribution of potential temperature and moisture (Ma and Bao, 2016). Figure 2 ((a) to (i)) shows the CAPE (shaded) along with equivalent potential temperature (theta; in ^{o} K) for all the three cases of PBL schemes and cyclones. The local scheme YSU overestimates CAPE values over a larger area of the Xynthia cyclone (Fig. 2d) while underestimates in case of Gong (Fig. 2g). The CAPE distributions are showing quite a variation among themselves and from one storm to other. On comprising, the amounts of CAPE in the two experiments were disparate corresponding to the observed CAPE of the storms. Almost all PBL schemes show dry bias from middle to upper troposphere (600 hPa–250 hPa), while YSU scheme carries this bias at the surface boundary layer, for all storms. Moreover, QNSE, UWMT and YMSU PBL schemes underestimate the tangential winds for these mid-latitude storms. The 24 h accumulated latent heat flux and precipitation from UWMT scheme show modified results as compared to YSU and QNSE PBL schemes.

This work is published in Climate Dynamics in 2019 [Impact Factor 4.048]

4.7 Demonstration of the temporal evolution of tropical cyclone "Phailin" using different cloud microphysical parameterization schemes

Introduction

The microphysical parameterization (MP) is an important source of uncertainty in numerical predication of mesoscale convective systems. Clouds associated with tropical cyclones (TCs) are typically organized into large rings and bands. TC's have clouds and precipitation structures similar to the mesoscale convective systems outside of the tropics. Therefore, similar to the problem of improving numerical weather prediction (NWP) models for quantitative precipitation forecasts, the problem of improving numerical TC forecasts is closely related to how to better simulate the impression of cloud microphysics on model-resolved winds, temperature, and moisture. The TCs are among the most important extreme weather phenomena in the tropics. Models skill predicting the TC track and intensity over the Bay of Bengal (BoB) have been discussed widely by previous studies. There are numerous MP schemes in Weather Research and Forecasting (WRF) Model and most of these schemes such as LIN explicit, WSM6, Thompson, WDM6, Thompson and Morrison, WSM 3-class simple ice and Ferrier have been widely used for TC forecast over North Indian Ocean.

During post monsoon, especially in month of October, the formation of depression to very severe cyclonic storms formation remain the highest and have quite impacts in Indian

subcontinent to Bangladesh, Myanmar, Sri Lanka, Oman, Somaliya, and Yeman. In the latest decade, the intensification of the number of cyclones over Indian Ocean has increased while the numbers of depressions have deceased. Few of the intensified and damaging (nearly in billions) by the cyclones were Gonu, Nargis, Giri, Thane, Phailin, Nilofar, Vardah, Ockhi, Mekunu, Fani, Kyarr and latest super cyclone Amphan in 2020 (IMD Archives: https://rsmcnewdelhi.imd.gov.in/report.php?internal_menu=MjY=). Since last few decades, two ESCSs (Odisha-1999, Phailin-2013) have made the landfall over Odisha coast. Both the VSCS occurred during post monsoon season and caused socio-economic damages and casualty of human-lives.

Results

The model used in this study is the Advanced Research WRF (ARW) version 3.6.1. The analyses and 6-hr forecast fields of the final analysis (FNL) of the NCEP at 1.0°x 1.0° grid space were taken as the initial and boundary conditions for the ARW model. The lateral boundary conditions are updated in 6-hr interval and the SST was kept constant throughout the model integration. The United States Geological Survey (USGS) data with 10min and 5min resolution were used to provide permanent land surface fields such as terrain/topography. A double domain of 25 km and 8.333 km were chosen, which extends from 75°–110° E and 4°–32° N with 42 vertical levels. The vertical levels are closely placed in the lower levels (12 levels below 850 hPa and 22 levels below 500 hPa) and are relatively coarser above. The model is integrated at a 3hrs interval using the Yonsei University (YSU) planetary boundary layer (PBL) scheme, Grell and Devenyi Ensemble (GDE) for convective parameterization scheme. Thus, GDE convective scheme used in this study.

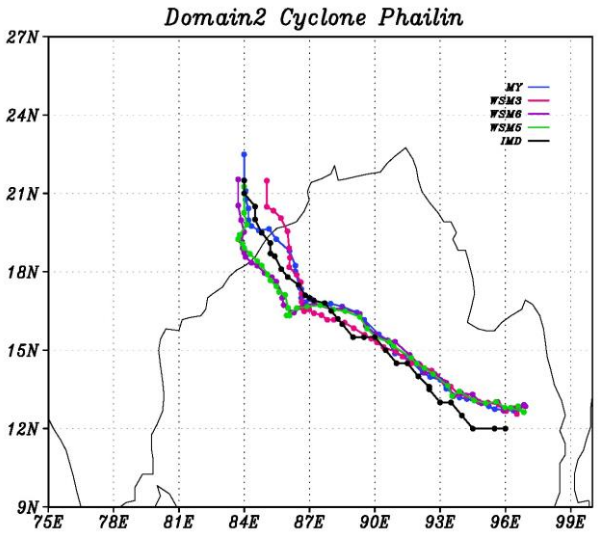

Fig. 1 Model simulated track positions of Phailin during 00 UTC 8 - 06 UTC 13 October 2013 using 00 UTC 08 October 2013 as initial conditions. The positions are identified through the minimum sea level pressure from different WRF experiments along with IMD observations.

The simulated track positions of Phailin from different MP experiments along with IMD observations are represented in Fig. 1. It is noticed that, all the MP experiments simulate slight deviation during the genesis stage of the Phailin. The simulated track positions from DD to VSCS are deviated to east and north of the IMD observation. However, later landfall of VSCS, positions of simulated tracks are west of the IMD observed track. From model experiments, initial location of the simulated tracks may have a shift than observations. The simulated track errors from the MP experiments from domain 1 (D01; 25 km) and domain 2 (D02; 8.333 km) resolutions indicates the sensitivity of tracks in terms of resolutions. The track errors during the simulations are found to vary as shown in Fig. 2(a) and (b). The 12-hours average track errors are lower in D02 as compared with D01, especially for MY scheme, which was expected from MP experiments; that may be due to changes in explicit moisture processes. Overall, among the four MP experiments, WSM3 scheme shown less errors than MY, WSM6 and WSM5 schemes during the simulations in both the domain.

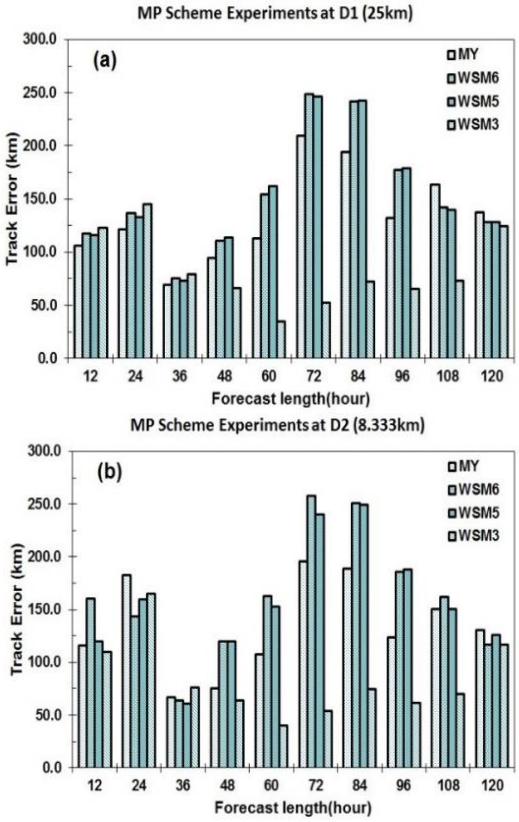

Fig. 2 Simulated track errors in 12-hrs average derived from different WRF experiments at (a) D01 and (b) D02 resolutions.

Impact of global warning on cyclones

Warming in the tropical Indian Ocean has increased at faster rate 0.15 ^{o}C/decade during 1951-2015 as compared to global ocean 0.11 ^{o}C/decade. They further added that this warming was non-uniform and ~90% of warming is attributed to anthropogenic activities (Roxy et al 2020). A change in the SST and moisture (specific humidity) for two decades that contributes positively to TC formation are shown in Figure 3 (a) and (b). The warming over western and central Indian Ocean, are one of few and prominent features of local warming. The availability of moisture in the atmosphere in the recent decade is an important aspect of the rapid intensification and strengthening of tropical cyclone before landfall (Fig 3b).

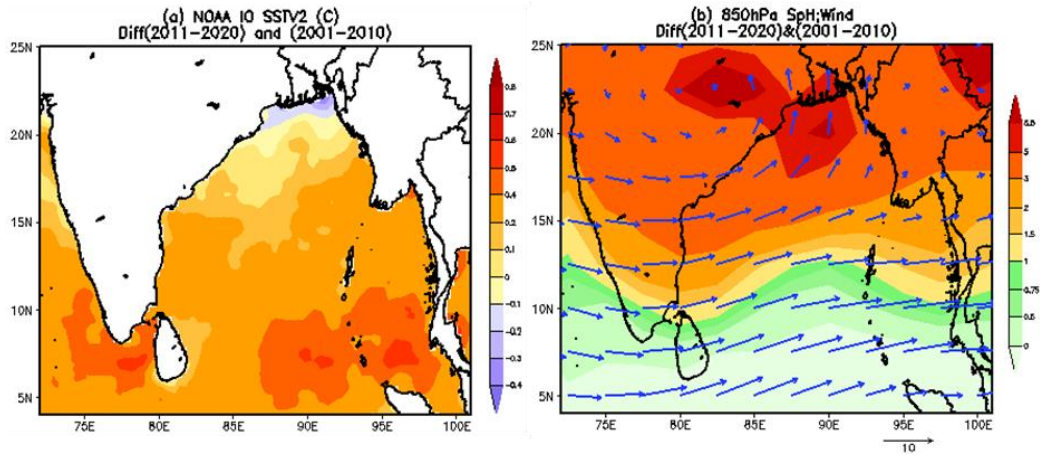

Fig. 3 : Variations of cyclone related varaibles over the BoB (a) Difference in SST (^{o}C) and (b) specific humidity (shaded; gm Kg^{-1}) along with wind (ms^{-1}) field at 850 hPa level during two recent decades 2011-2020 and 2001-2010 derived from NOAA renalysis.

Table 1: Decadal variability of number of tropical storms over the Bay of Bengal during month Oct-Nov, 2001-2020.

Year			DD	*SCS	ESCS	Duration of ESCS ≥ 24 hours
2001-2010	20	14	2		2	
2011-2020	19	11	6		6	

*SCS = SC +SCS; DD= Deep Depression; SCS = Severe Cyclonic Storms

Under global warming scenario there may be other reasons of the rapid intensification of storms before landfall, yet SST, and moisture supply are two driving factors over Indian Ocean. However, we found SST and moisture supply are the one of the main component of rapid intensification of cyclones over Bay of Bengal. Table-1 shows formation of the total number of low-pressure systems over Bay of Bengal and Arabian Sea during October-November in last 20 years (2000-2020). There were large variations in the number of cyclones formation in the first decade 1991-2000. The depressions are decreased since while severe cyclones have increased. Furthermore, due to warming the intensity of the land-falling cyclones from severe to very severe cyclonic storm (SCS/VSCS) escalated 24hrs before landfall. The numbers of such cyclones have increased 3 times during 2011-2020 as compared to 2001-2010 over the Bay of Bengal. Such changes are attributed to enhance in the necessary and sufficient condition of the cyclone formations in the region, which includes supply of abundant moisture supply and warmer SST in the recent years (Figure-4). The comparison of SST, moisture and winds in recent two decades shows the favorable conditions, those facilitated the formation of VSCS. Table-2 shows the details of the VSCS cyclones formation in recent two decades.

This work is published in Ocean MPDI, 2021, Page 648–674

4.8 Stratospheric sudden warmings observed in the last decade by using GPSRO, other satellite and reanalysis measurements

Introduction

A sudden stratospheric warming (SSW) is a dramatic event that occurs during the winter in the middle atmosphere which changes temperature and wind circulation in a short period. In addition, SSW is now recognized as one of the strongest manifestations of the dynamical coupling of the troposphere-stratosphere system with effects seen up to the mesosphere and lower thermosphere (MLT)/ionosphere. The cause for SSW is attributed to the propagation of atmospheric waves (mainly planetary waves, PWs), which regulates the dynamics in stratosphere and mesosphere. The present study evaluate the impact of SSW events which occurred in the last decade (2002-2013) on the latitudinal variation of the tropopause, stratopause, and mesopause characteristics including the gravity wave (GW) activity by using multi-satellite (Global Positioning System Radio Occultation (GPS RO), Microwave Limb Sounder (MLS), Sounding of the Atmosphere using Broadband Emission Radiometry (SABER)) and reanalysis (European Centre for Medium-Range Weather Forecasts (*ECMWF*) ERA-Interim and Geostationary Operational Environmental Satellite system (GOES-5)) datasets.

Results

SSWs have been classified into major and minor warmings depending on the amplitude and location of the temperature perturbations. According to the World Meteorological Organization (WMO) definition,

major SSWs are identified when the zonal mean wind at 10-hPa (~30 km) moves poleward of 60^{o}N and reverses from eastward to westward.

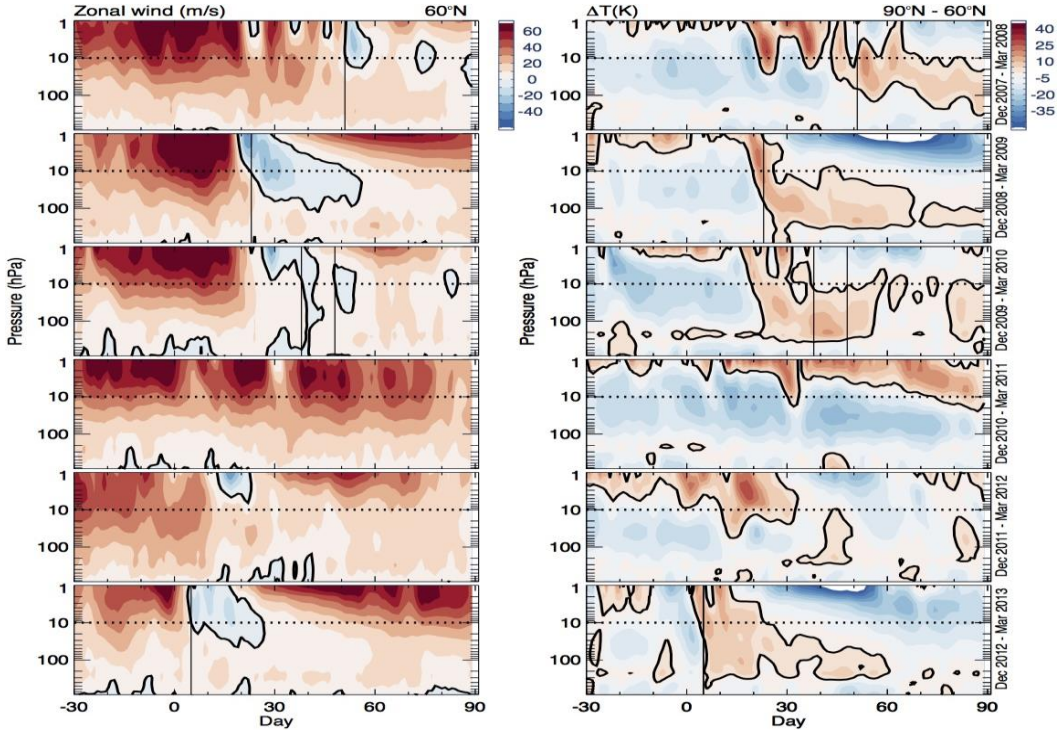

Fig. 1 Time-height section of zonal mean zonal wind (left panels) at 60^{o}N and the temperature gradient (right panels) between 60^{o}N and the north pole observed during 1 December (-30th day) to 31 March (90th day) for 2001 to 2007 winter periods using ERA-Interim re-analyses. Eastward winds and positive temperature gradients are shaded with red color. The dotted horizontal line indicates the 10-hPa level. The black vertical line represents the first day of the warming. The contour interval is 5 m/s and 5 K for zonal wind and temperature, respectively.

In addition to the reversal of the winds at 10-hPa over 60^{o}N, the 10-hPa zonal mean temperature gradient between 60^{o}N and 90^{o}N should also be positive which was described in Fig 1. By using temperature profile the WMO defines the (first) tropopause as the lowest level at which the lapse rate decreases to 2^{o}C/km or less, provided also the average lapse rate between this level and all higher levels within 2 km does not exceed 2^{o}C/km. Similarly stratopause and mesopause are identified at the altitudes where maximum and minimum temperatures exist, respectively. Fig 2 shows the zonal-mean stratopause altitude (left panels) and temperature (right panels) during 2008-2009 and 2012-2013 winter from MLS measurements. As mentioned earlier, the stratopause altitude is defined as the warmest temperature point between 40 and 80 km. During December in all winters, the stratopause altitude at high-latitudes (60-80^{o}N) is constant around 55-60 km and decreases when SSW starts developing. During the SSW period, the stratopause altitude reaches as high as ~75 km with temperatures ranging between 230-240 K, which is much cooler than the non-warming year, where stratopause temperatures range from 255-265 K.

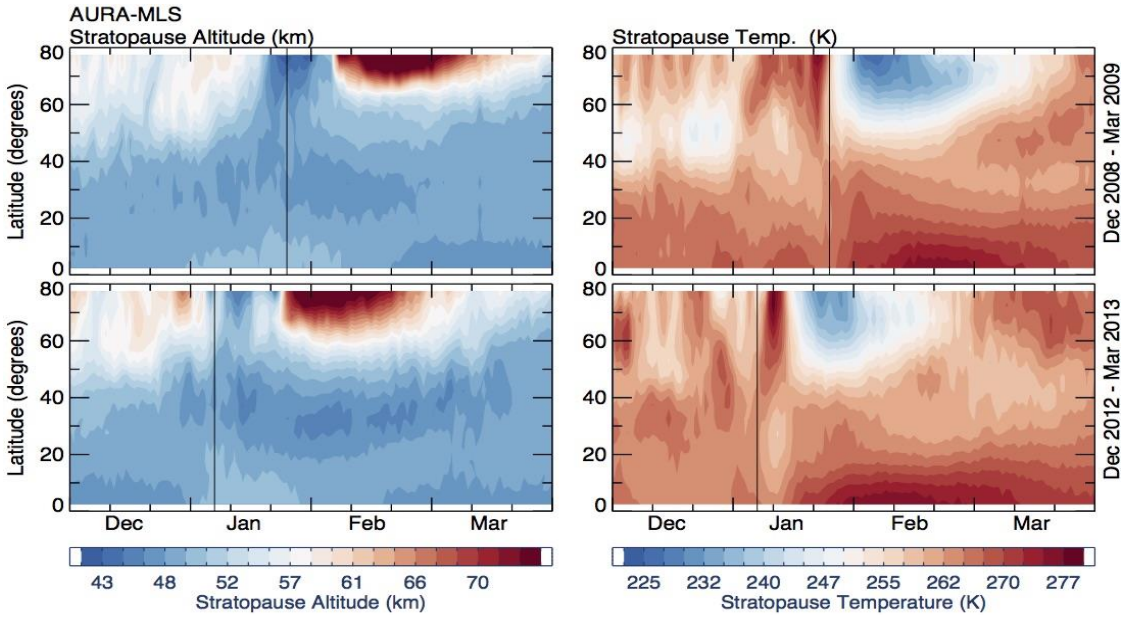

Fig 2 Latitude-time contours of stratopause altitudes (left panels) and temperatures (right panels) observed using MLS satellite measurement during 2008-2009 and 2012-2013 warming winters, respectively. The vertical black line indicates the beginning of the warming period.

Latitude-time structures of mesopause altitude and temperatures observed using SABER satellite measurements during 2008-2009 and 2012-2013 winter periods are shown in Fig 2. The blank areas in Fig 10 represent the data gaps due to the latitudinal coverage of SABER, which switches between the NH viewing phase and the SH viewing phase approximately every 60 days. During the onset or before the SSW event, we observe the mesopause at approximately 92 km altitude at 80^{o}N latitude in 2008-2009, and 2012-2013 winters. A mesopause altitude seems to decline for about ~3-4 km below the mean mesopause altitude during SSW periods. Gravity wave energy (*Ep*) observed is almost 4 times during warming year when compared to non-warming years. Thus, enhanced GW activity during warming years is somehow related to the SSW event.

5. List of Publications

Research Papers published in International Journals during (2017 to 2021) in collaboration with NARL, Gadanki, Department of Space, Govt. of India

1. Ramesh, K., S. Sridharan, K. Raghunath, and **S. V. B. Rao** (2017), A chemical perspective of day and night tropical(10°N–15°N) mesospheric inversion layers, *J. Geophys. Res. Space Physics*,122, doi:10.1002/2016JA023721. **Impact factor: 3.426.**
2. Kishore, Isabella Velicogna, M. VenkatRatnam, S. P. Namboothiri, J. H. Jiang, Tyler C Sutterley, V. Sivakumar, **G. N. Madhavi**, and **S. V. B. Rao** (2016). Sudden Stratospheric warming's observed in the last decade by satellite measurements and reanalysis: Remote Sensing Of Environment, 184, Pages: 263-275, **Impact Factor : 5.881.**
3. S. Eswaraiah, G. Venkata Chalapathi, K. Niranjan Kumar, M. Venkat Ratnam, Yong Ha Kim, P. Vishnu Prasanth, Jaewook Lee, **S.V.B. Rao,** (2018) A case study of convectively generated gravity waves coupling of the lower atmosphere and mesosphere-lower thermosphere (MLT) over the tropical region: An observational evidence. *J. Atmospheric and Solar Terrestrial Physics*, DOI: 10.1016/j.jastp.2018.01.005. **Impact Factor: 1.492**
4. K. Vijayakumar, P. C. S. Devara, David M. Giles, Brent N. Holben, S. Vijaya Bhaskara Rao & C. K. Jayasankar, (2018), Validation of satellite and model aerosol optical depth and precipitable water vapour observations with AERONET data over Pune, India. *International Journal of Remote Sensing*, DOI: 10.1080/01431161.2018.1476789.
5. M. Venkat Ratnam, P. Prasad, M. Roja Raman, V. Ravikiran, **S. V. B. Rao**, B.V. Krishna Murthy, A. Jayaraman, (2018) Role of dynamics on the formation and maintenance of the elevated aerosol layer during monsoon season over southeast peninsular India. *Atmospheric Environment*, DOI:10.1016/j.atmosenv.2018.06.023. **Impact Factor: 3.948**
6. S Eswaraiah, Yong Ha Kim, Jaewook Lee, M Venkat Ratnam, **S.V.B. Rao,** (2018) Effect of Southern Hemisphere sudden stratospheric warmings on Antarctica mesospheric tides: First observational study. *J. Geophys. Research: Space Physics*, DOI: 10.1002/2017JA024839. **Impact Factor: 3.426**
7. PP Sreekala, **S V B Rao**, K Rajeevan, MS Arunachalam, (2018) Combined effect of MJO, ENSO and IOD on the intraseasonal variability of northeast monsoon rainfall over south peninsular India. *Climate Dynamics*, DOI: 10.1007/s00382-018-4117-3. **Impact Factor: 4.708**
8. G. Venkata Chalapathi, S. Eswaraiah, M. Venkat Ratnam, K. Niranjan Kumar, P.Vishnu Prasanth, Jaewook Lee, Yong Ha Kim, **S.V.B. Rao** (2018) Stratosphere mesosphere Coupling Through Vertically Propagating Gravity Waves During Mesospheric Temperature Inversion (MTI): An Evidence. *IJCRR*, DOI: 10.7324/IJCRR.2018.1011. **Impact Factor: 4.016**
9. P.K. Pradhan, Margarida L.R. Liberato, Juan A. Ferreira, S. Dasamsetti, **S. V. B. Rao** (2017) Characteristics of different convective parameterization schemes on the

simulation of intensity and track of severe extratropical cyclones over North Atlantic. *Atmospheric Research.* DOI:10.1016/j.atmosres.2017.09.007. **Impact Factor: 3.817**

10. **Vijaya Kumari K**, Sagar S K, Yesubabu V, Hari Prasad D, **S. Vijaya Bhaskar Rao** (2018) Role of Planetary Boundary Layer Processes in the Simulation of Tropical Cyclones Over the Bay of Bengal. *Pure and Applied Geophysics* 176 (2), 951-977.
11. Pramitha, M & kishore kumar, Karanam & Madineni, Venkat Ratnam, **S. Vijaya Bhaskar Rao** (2019). Meteor radar estimation of Gravity Wave Variances and Momentum Fluxes in the mesosphere lower thermosphere: Evaluation of different methods using simulations and observations over three tropical locations. 1-4. 10.23919/URSIAP-RASC.2019.8738324.
12. Eswaraiah S, Venkat Ratnam M, Yong HaKim, Kondapalli NiranjanKumar, Venkata Chalapathi G, **Ramanajaneyulu L**, JaewookLee, Vishnu Prasanth P, Thyagarajan K, **S. Vijaya Bhaskar Rao** (2019) Advanced meteor radar observations of mesospheric dynamics during 2017 minor SSW over the tropical region. *Advances in Space Research*, https://doi.org/10.1016/j.asr.2019.05.039
13. **P. K. Pradhan,** Margarida L. R. Liberato, Vinay Kumar, **S. Vijaya Bhaskar Rao**, Juan Ferreira, Tushar Sihna (2019) Simulation of Mid-latitude Cyclones over North Atlantic Ocean: Impact of Boundary Layer Parameterization Schemes. *Climate Dynamic*, Volume 53 (11), Page 6785–6814.https://doi.org/10.1007/s00382-019-04962-3
14. Kattamanchi, Vijaya Kumari, Yesubabu Viswanadhapalli, Hari Prasad Dasari, Sabique Langodan, Naresh Krishna Vissa, Sivareddy Sanikommu, and **S. Vijaya Bhaskara Rao**. "Impact of assimilation of SCATSAT-1 data on coupled ocean-atmospheric simulations of tropical cyclones over Bay of Bengal." *Atmospheric Research* 261 (2021): 105733.
15. Yesubabu, Viswanadhapalli, Vijaya Kumari Kattamanchi, Naresh Krishna Vissa, Hari Prasad Dasari, and **S. Vijaya Bhaskara Rao** "Impact of ocean mixed-layer depth initialization on the simulation of tropical cyclones over the Bay of Bengal using the WRF-ARW model." *Meteorological Applications* 27, no. 1 (2020): e1862.
16. Vinay Kumar, P. K. Pradhan, Tushar Sinha, **S Vijaya Bhaskara Rao**, Hao- Po Chang (2020): An interaction of low-pressure system, off-shore trough and mid-tropospheric dry air intrusion: Kerala flood August 2018. *MDPI Atmosphere,11,740, Page 1-21* https://doi.org/10.3390/atmos11070740
17. P. K. Pradhan**,** Vinay Kumar, Sunilkumar Khadgarai, **S. Vijaya Bhaskara Rao**, Tushar Sinha, K. VijayaKumari, Sandeep Pattnaik (2021) Demonstration of the temporal evolution of tropical cyclone "Phailin" using different cloud microphysical parameterization schemes. MDPI Ocean (2) Page 648–674. https://doi.org/10.3390/oceans2030037
18. P. K. Pradhan, D. Hari Prasad, D. Srinivas, **S. Vijaya Bhaskara Rao**, Guvvala. Rambabu (2021): Sensitivity of Initial and Boundary Conditions on the Simulation of Track and Intensity of Extratropical Cyclone 'Gong' over North Atlantic. *Journal of Earth System Science,136(46) Page 1-21* https://doi.org/10.1007/s12040-020-01546-2

Papers presented in National/International workshops/conferences

1. Study on the Role of Planetary Boundary Layer Process in simulation of Post Monsoon Tropical cyclones over Bay of Bengal. **K.Vijaya Kumari**, S. Karuna Sagar, V. YesuBabu and S. Vijaya Bhaskara Rao, 19th National Space Science Symposium, VSSC , Tiruvananthapuram, 9-12 February, 2016
2. Planetary wave characteristics revealed by SVU Meteor Radar over Tiruapti: Comparison with SKY MET Radar at Thumba.- Poster **L. Ramanjaneyulu**, M. Venkat Ratnam, S. Eswaraiah, K. Kishore kumar, K.V. Subhrahmanyam and S. Vijaya Bhaskara rao. ***Best Poster Award NSSS-2016, VSSC, Tiruvananthapuram.***
3. The ultra-fast and fast kelvin waves in the equatorial Mesosphere and Lower Thermosphere region. **G. N. Madhavi**, P. Kishore and S.Vijaya Bhaskara Rao ,19th National Space Science Symposium, VSSC , Tiruvananthapuram, 9-12 February, 2016.
4. Impact of Planetary Boundary Layer Process in simulation of Post Monsoon Tropical cyclones over Bay of Bengal. Poster. **K. VijayaKumari**, S. KarunaSagar , V. Yesubabu, **S.V.B. Rao,** 104th Indian Science Congress, S.V.University, Tirupati, 3-7 January 2017.
5. Planetary wave characteristics revealed by SVU Meteor Radar over Tiruapti: Comparison with SKY MET Radar at Thumba.- Poster **L. Ramanjaneyulu**, M. Venkat Ratnam, S.Eswaraiah, K. Kishore kumar, K.V. Subhrahmanyam and S. Vijaya Bhaskara rao. 104th Indian Science Congress, S.V.University, Tirupati, 3-7 January 2017.
6. Impact of Microphysical Parameterization Schemes on Phailin Simulation over Bay of Bengal, **P. K. Pradhan**, S. Pattnaik, **K. Vijaya Kumari** and **S. V. B. Rao**, 104th Indian Science Congress (Earth System Sciences), Sri Venkateswara University, Tirupati, January 03-07, 2017.
7. A case study of mesospheric fast and ultrafast Kelvin waves observed over a three-radar network using Empirical Mode Decomposition. P. Kishore, Isabella Velicogna, Yara Mohajerani, Enrico Ciraci, G.N.Madhavi and SVBRAO, 104th Indian Science Congress, Sri Venkateswara University, Tirupati, January 03-07, 2017.
8. Variability and Predictability of Indo-Pacific SST and its Influence on North East Monsoon Rainfall over South Peninsular India. **P. K. Pradhan**, Venkatraman Prasanna, **S. Vijaya Bhaskara Rao** and Vinay Kumar, Understanding, Predicting and Projecting Climate Change over Asian Region (UPCAR), Sri Venkateswara University-NARL, June 26-28, 2017.

9. **P. K. Pradhan,** K. Vijaya Kumari, S. Vijaya Bhaskara Rao (2020) Simulation of Monsoon Depression over Coastal Odisha during 15-17 August, 2018 at National Conference on Coastal Ocean-Atmosphere Science and Technology (COAST-2020), Berhampur University, Odisha during 28 Feb-01 Mar 2020.
10. **P. K. Pradhan,** Vinay Kumar, Karuna Sagar, S. Vijaya Bhaskara Rao, N. Shalini (2019) Synoptic rain-bearing systems associated with Kerala flood event during 13-18 August 2018 by at International Symposium on Advances in Coastal Research with special reference to Indo-Pacific- 2019 (AdCoRe IP 2019), MoES-NCCR during 17-19 December, **2019**.

National/International Workshop and Schools attended by the scholars

1. APSCIENCECONGRESS.27-29, January 2016, S.V.University, Tirupati, A.P.
2. NSSS-2016, February 9-12, VSSC, Kerala.
3. Indian Science Congress, Tirupati, Jan 3-7, 2017.
4. SPARC General Assembly-2018, Miyakomessie, Kyoto, Japan, October 1-5, 2018.
5. Workshop on **"Satellite Navigation & Applications of GNSS/NavIC"** held at National Atmospheric Research Laboratory, Gadanki, Department of Space (Govt. of India) during 5-6 April 2018.
6. The international and interdisciplinary PhD and Post-Doc Winter School (IAWS18) entitled **"The Arctic Ocean: atmosphere, ice and ocean interactions– implications for future climate and human activities (Theory and Practical Classes on Polar Research)"** held at National Centre for Polar Ocean Research (NCPOR), Goa during October 28-02 November 2018.
7. SERB school on "**Numerical Modelling and Forecasting of Desert Storm and Cloud burst (NUMCLOUDS)"** sponsored by Department Science and Technology, (Govt. of India) held at Department of Atmospheric Science, Central University of Rajasthan (CURaj), India from 11-23 February, 2019
8. URSI RCRS 2020, IIT (BHU), Varanasi, India, 12 - 14 February, 2020.